

# Negative differential conductance induced by spin-charge separation.

F. Cavaliere<sup>1</sup>, A. Braggio<sup>1</sup>, J. T. Stockburger<sup>2</sup>, M. Sassetti<sup>1</sup>, and B. Kramer<sup>3</sup>

<sup>1</sup> *Dipartimento di Fisica, INFN-Lamia, Università di Genova, Via Dodecaneso 33, 16146 Genova, Italy*

<sup>2</sup> *II. Institut für Theoretische Physik, Universität Stuttgart, Pfaffenwaldring 57, 70550 Stuttgart, Germany*

<sup>3</sup> *I. Institut für Theoretische Physik, Universität Hamburg, Jungiusstraße 9, 20355 Hamburg, Germany*

(Dated: May 04, 2004)

Spin-charge states of correlated electrons in a one-dimensional quantum dot attached to interacting leads are studied in the non-linear transport regime. With non-symmetric tunnel barriers, regions of negative differential conductance induced by spin-charge separation are found. They are due to a correlation-induced trapping of higher-spin states without magnetic field, and associated with a strong increase in the fluctuations of the electron spin.

PACS numbers: 73.63.Kv, 71.10.Pm, 73.22.Lp

In single electron transport [1], the electron charge causes the Coulomb blockade effect that stabilizes the electron number in a device. Experiments show also that the electron spin can lead to important mesoscopic transport effects. For instance, quantum dots in carbon nanotubes [2, 3, 4] have revealed several non-equilibrium and coherent spin processes, and spin-parity effects.

For few-electron quantum dots, the spin blockade effect has been predicted [5]. In one dimension (1D) this is indicated by a negative differential conductance that occurs *only* when a state with maximum spin value is occupied. Combining spin blockade with spin-polarized detection, the electron spin in a 2D-lateral quantum dot was probed [6]. Also, in a few-electron vertical quantum dot higher-spin states, not directly accessible from the ground state, were detected via probing with non-equilibrium voltage pulses [7]. When spin relaxation was absent, strong fluctuations of spin and charge were observed. Motivated by experiments on a quasi-1D quantum dot formed by two impurities in a quantum wire [8], we have calculated microscopically single electron transport through a 1D quantum dot formed by two equal tunnel barriers in a Tomonaga-Luttinger liquid. Signatures of non-Fermi liquid behavior and, in the presence of a magnetic field, correlation-enhanced spin polarization were found [9]. Spin-charge separation has been observed [10] and analyzed theoretically [11] in tunneling between parallel quantum wires. In the *coherent* tunneling regime, the effects of non-Fermi liquid correlations in 1D quantum dots have been investigated non-perturbatively [12, 13].

In the present work, we consider a 1D quantum dot in the incoherent sequential tunneling region. We predict that states with higher total electron spin in a non-magnetic 1D quantum dot containing an *arbitrary* number of electrons can be dynamically stabilized by tuning the asymmetry of tunnel barriers. The occupation of these states can lead, in the sequential tunneling regime, to a negative differential conductance. This is caused by the peculiar nature of the *non-Fermi liquid correlations* that determine the tunneling rates. The new phe-

nomenon is due to *spin-charge separation* and is different from the previously discussed negative conductance associated with spin selection rules via Clebsch-Gordan coefficients that were included in the tunneling rates *ad hoc* [5]. We study the combined effects of asymmetry, electron correlations and relaxation. We predict that stabilization of the higher-spin states is associated with a strong increase of the spin fluctuations. Relaxation of these states strongly affects the negative differential conductance, in contrast to “normal” states associated with positive conductances. Our results open a novel possibility of experimentally addressing non-Fermi liquid behavior without performing often cumbersome analyses of temperature dependences.

We start from the microscopic Hamiltonian  $H = H_d + H_l + H_t$ , which contains the dot ( $H_d$ ), the leads ( $H_l$ ), and a tunneling term ( $H_t$ ). The dot is modeled as an interacting 1D system confined to  $|x| < d/2$ , with excitations associated with *independent* energy scales [9]

$$H_d(n, s, \rho, \sigma) = \frac{E_\rho}{2}(n - n_g)^2 + \frac{E_\sigma}{2}s^2 + \rho\varepsilon_\rho + \sigma\varepsilon_\sigma. \quad (1)$$

Here,  $n$  and  $s$  represent the number of electrons, measured relative to the number of charges  $n_g$  corresponding to a gate voltage  $V_g$ , and the  $z$ -component of the total spin in units of  $\hbar/2$ , respectively. Energy scales  $E_\rho$  and  $E_\sigma$  are the charge and spin addition energies. The last two terms do not change the total charge and spin but describe intra-dot charge and spin density waves, where  $\rho$  and  $\sigma$  are related to bosonic creation and annihilation operators via  $\rho = \sum_j j b_{\rho,j}^\dagger b_{\rho,j}$  and  $\sigma = \sum_j j b_{\sigma,j}^\dagger b_{\sigma,j}$ .

The energy parameters in Eq. (1) reflect the microscopic electron interaction parameterized by [14]

$$g_\rho^2 = \frac{1 + V_x}{1 - V_x + 4V_0}, \quad g_\sigma^2 = \frac{1 + V_x}{1 - V_x}, \quad (2)$$

with the exchange and Coulomb matrix elements  $V_x = \hat{V}(2k_F)/2\pi\hbar v_F$  and  $V_0 = \hat{V}(q=0)/2\pi\hbar v_F$ , respectively. In experiment, the charging energy is not solely influenced by the microscopic interaction in the quantum

dot. Therefore, we treat it as an independent parameter, typically  $E_\rho \gg E_\sigma$ . The spin addition energy,  $E_\sigma = \pi\hbar v_\sigma/2dg_\sigma$ , is due to the Pauli principle. The excitation energies of the neutral charge and spin modes are  $\varepsilon_\nu = \pi\hbar v_\nu/d$  with charge and spin mode velocities  $v_\nu = v_F(1 + V_x)/g_\nu$  ( $\nu = \rho, \sigma$ ). Without interaction,  $g_\rho = g_\sigma = 1$ , we have  $E_\sigma \equiv E_0 = \pi\hbar v_F/2d$  and  $\varepsilon_\rho = \varepsilon_\sigma = 2E_0$ . We assume the leads to be Luttinger liquids with Coulomb repulsion  $g_0 \leq 1$ , low-energy charge and spin mode dispersions  $\omega_\rho(q) = v_F|q|/g_0$  and  $\omega_\sigma(q) = v_F|q|$ . We assume  $g_0 \neq g_\rho$ , since the interaction can differ between dot and leads. Tunneling between the leads and the dot at  $x = \pm d/2$  is described by  $H_t$  with amplitudes  $\Delta_l$  and  $\Delta_r$ . We consider weak tunneling [9].

For not too low temperatures,  $k_B T \gg \delta E$ , transport is dominated by incoherent sequential tunneling and one can safely neglect higher order coherent processes [15]. Here,  $\delta E$  represents the level broadening due to higher order contribution from tunneling via virtual states, and is proportional to the rate  $\gamma$  in Eq. (4). The kinetic variables are then  $n$  and  $s$  only since  $\rho$  and  $\sigma$  relax towards thermal equilibrium very efficiently due to mechanisms such as coupling to phonons and spin-orbit interaction. The opposite limit, but for the spinless case, has been considered in [16]. The relaxation of the spin  $s$ , which is effected by the same processes as well as co-tunneling, is usually much slower [17]. Therefore, both tunneling and spin relaxation have to be included in the Master equation. In order to be able to resolve the spin dynamics we consider  $k_B T < E_\sigma$ . In the stationary limit, one has to solve  $\sum_{\eta'} [P(\eta')\Gamma^{\eta' \rightarrow \eta} - P(\eta)\Gamma^{\eta \rightarrow \eta'}] = 0$  for the probabilities  $P(\eta) \equiv P(n, s)$ . Tunneling is characterized by rates  $\Gamma_{r,l}^{\eta \rightarrow \eta'}$ , subject to the selection rules  $n' = n \pm 1$ ,  $s' = s \pm 1$ . These contain the non-Fermi liquid correlations and can be calculated microscopically for finite temperature [9]. For simplicity, we quote only the expression for  $T = 0$

$$\Gamma_{r,l}^{i \rightarrow j}(E_{i \rightarrow j}) = \gamma_{r,l} \sum_{\rho, \sigma \geq 0} a_\rho a_\sigma \left( \frac{X_{\rho, \sigma}^{i,j}}{\hbar\omega_c} \right)^\alpha \Theta(X_{\rho, \sigma}^{i,j}), \quad (3)$$

with  $X_{\rho, \sigma}^{i,j} = E_{i \rightarrow j} - \rho\varepsilon_\rho - \sigma\varepsilon_\sigma$ ,  $\alpha = (1/g_0 - 1)/2$ ,  $a_\nu = \Gamma(1/2g_\nu + \nu)/\Gamma(1/2g_\nu)\nu!$  and the intrinsic rates

$$\gamma_{r,l} = \left( \frac{\varepsilon_\rho}{\hbar\omega_c} \right)^{1/2g_\rho} \left( \frac{\varepsilon_\sigma}{\hbar\omega_c} \right)^{1/2g_\sigma} \frac{\hbar\omega_c G_{r,l}}{e^2 \Gamma(1 + \alpha)}, \quad (4)$$

with  $\omega_c$  the cutoff frequency [14],  $G_{r,l} = (\pi e \Delta_{r,l}/\omega_c)^2/h$  the tunneling conductances, and  $E_{i \rightarrow j}$  obtained from the charge and spin addition energies corresponding to the states  $i$  and  $j$ . The neutral spin and charge modes (energy scales  $\varepsilon_\rho$  and  $\varepsilon_\sigma$ ) are fully taken into account. For the spin relaxation, obeying the selection rules  $s' = s \pm 2$  and  $n' = n$ , we use the detailed-balance result

$$\Gamma_{\text{rel}}^{s \rightarrow s'} = \begin{cases} w & |s'| < |s| \\ w \exp[-\frac{1}{2}\beta E_\sigma (s'^2 - s^2)] & |s'| > |s| \end{cases} \quad (5)$$

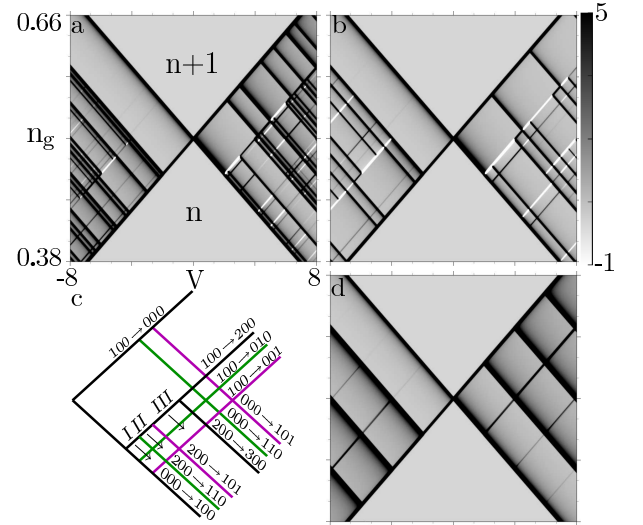


FIG. 1: Differential conductance at  $k_B T = 10^{-2} E_\sigma$  in the  $(V, n_g)$ -plane with asymmetry  $A = 100$ , interaction strength in the leads  $g_0 = 0.9$ , charging energy  $E_\rho = 25 E_\sigma$ , and spin relaxation  $w = 0$  ( $V$  in units of  $E_\sigma/e$ ); (a)  $\varepsilon_\rho = 3.0 E_\sigma$ ,  $\varepsilon_\sigma = 2.2 E_\sigma$ ; (b)  $\varepsilon_\rho = 15 E_\sigma$ ,  $\varepsilon_\sigma = 2.5 E_\sigma$ ; (c) states involved in the transitions for  $V > 0$  near the linear conductance peak, and denoted by the triples of integer quantum numbers  $(s, \sigma, \rho)$ ; (d) non-interacting case,  $\varepsilon_\rho = \varepsilon_\sigma = 2 E_0$ . Right edge: grey scale in arbitrary units, labels and scales in a,b,d are identical.

containing a phenomenological rate  $w$ , and  $1/\beta \equiv k_B T$ .

Numerical results for the differential conductance  $G$  in the plane of bias  $V$  and gate voltage  $V_g \propto n_g$  are shown in Fig. 1 for  $g_0 = 0.9$ ,  $w = 0$ ,  $k_B T = 10^{-2} E_\sigma$ , and non-symmetric barriers near a charge transition  $n \leftrightarrow n+1$  ( $n$  even). The asymmetry  $A = G_l/G_r$  has been assumed to be large, and the temperature low, in order to emphasize also weaker features in the conductance. The intersection points at the centers of the grey-scale panels ( $n_g = n_{\text{res}}$ ,  $V = 0$ ) denote a linear conductance peak. The grey areas denote the Coulomb blockade regions. Black and white lines for  $V \neq 0$  correspond to positive and negative differential conductance peaks, respectively. Here, transitions involving additional spin states as well as neutral spin or charge modes in the quantum dot become relevant (Fig. 1c). Remarkably, it is the spin-charge separation in the dot that induces negative conductance peaks which separate certain spin states. Independently of the asymmetry  $A$ , these features are *not* present when spin-charge separation is removed, i.e.  $\varepsilon_\rho = \varepsilon_\sigma = 2 E_0$  (Fig. 1d).

In order to understand the physics behind the negative differential conductances we concentrate in the following on the regions denoted as I, II and III (Fig. 1c). Here, for  $k_B T < E_\sigma$ , only the five states  $\eta = (n, s = 0)$ ,  $(n+1, s = \pm 1)$ ,  $(n, s = \pm 2)$  are necessary to obtain a good approximation for the conductance. We assume  $A > 1$  and that the electrons flow from right to left for  $V > 0$ . Then, the quantum dot with lower particle number  $n$

will have a higher occupation probability. This implies that negative conductances can only occur parallel to the transition line  $(100) \rightarrow (000)$ , see Fig. 1c.

Using this model, the Master equation can be solved analytically using the rates from Eqs. (3)-(5) and the energies  $E_{0 \rightarrow 1} = eV/2 + E_\rho(n_g - n_{\text{res}})$ ,  $E_{2 \rightarrow 1} = E_{0 \rightarrow 1} + 2E_\sigma$  and  $E_{1 \rightarrow 0} = eV - E_{0 \rightarrow 1}$ ,  $E_{1 \rightarrow 2} = eV - E_{2 \rightarrow 1}$ . The current  $I(V)$  can be evaluated, and from that  $G = \partial I / \partial V \equiv N/D$ . Keeping only the dominant terms near the transition lines parallel to  $(100) \rightarrow (200)$ , with  $g_0 \approx 1$ , one obtains  $D = [\Gamma_1^{1 \rightarrow 0} \Gamma_r^{2 \rightarrow 1} + 2\Gamma_r^{0 \rightarrow 1} (\Gamma_r^{2 \rightarrow 1} + \Gamma_1^{1 \rightarrow 2}) + w(\Gamma_1^{1 \rightarrow 0} + \Gamma_1^{1 \rightarrow 2} + 2\Gamma_r^{0 \rightarrow 1})]^2 > 0$  and the numerator

$$N = e\vartheta \Gamma_r^{0 \rightarrow 1} \sum_{p=\pm 1} [\vartheta K_1^{(p)} + \delta K_2^{(p)}] \quad (6)$$

with  $\vartheta = 2(w + \Gamma_r^{2 \rightarrow 1})$ ,  $\delta = \Gamma_r^{2 \rightarrow 1} - 2\Gamma_r^{0 \rightarrow 1}$  and

$$K_1^{(p)} = \Gamma_r^{0 \rightarrow 1} \frac{\partial \Gamma_1^{1 \rightarrow 1+p}}{\partial V}; K_2^{(p)} = p \Gamma_1^{1 \rightarrow 1-p} \frac{\partial \Gamma_1^{1 \rightarrow 1+p}}{\partial V}. \quad (7)$$

From Eqs. (6) and (7) one recognizes that for obtaining a negative differential conductance one needs  $N < 0$ . This implies  $\delta \sum_p K_2^{(p)} < -\vartheta \sum_p K_1^{(p)}$  since  $\vartheta \sum_p K_1^{(p)}$  is always positive. From Eq. (3) one finds that the rate changes depend crucially on the presence and strengths of the correlations via  $a_\nu$ . Without correlations ( $g_0 = g_\rho = g_\sigma = 1$ ), the rates are integer multiples of  $\gamma_{r,1}$ . In particular, one finds  $\Gamma_r^{2 \rightarrow 1} = 2\Gamma_r^{0 \rightarrow 1}$  such that *always*  $G \geq 0$  (Fig. 1d), even in the most favorable limit  $A \rightarrow \infty$  and  $w = 0$ . This suggests that it is the influence of the intra-dot non-Fermi liquid correlations on the rates which yields the negative differential conductance.

To support this we introduced correlations in the dot ( $g_\sigma > 1$ ,  $g_\rho < 1$ ) while keeping the leads non-interacting ( $g_0 = 1$ ), for  $w = 0$  and  $A \rightarrow \infty$ , with a fixed  $G_r$ . One finds that along the line  $(100) \rightarrow (200)$  one has  $K_2^{(1)} > 0$ , and  $K_2^{(-1)} = 0$ . This implies *always* negative conductance in I and II since  $\delta < 0$ . The state  $(200)$  acts as a bottleneck for the current, since it cannot relax to the ground state via a single tunneling event. It accumulates probability at the expense of  $(000)$ . In region III, due to the additional activation of the charge wave state  $(101)$  in  $\Gamma_r^{2 \rightarrow 1}$ , depending on  $a_{\sigma=1} + a_{\rho=1} \leq 1$  one has  $\delta \leq 1$  and the conductance can be both negative and positive. However, for interactions with  $V_0 > 2V_x$  one always gets  $G > 0$ . In Fig. 1b, region III is absent due to  $g_\rho \ll 1$  (strong correlation). Therefore, we find only negative conductance as long as  $(300)$  does not contribute. Similarly, one can analyze the conductance associated with higher quantum numbers  $(s, \sigma, \rho)$ . In all of the cases analyzed we have found that the *necessary* ingredient for negative conductance is the spin-charge separation. In order to show that the states with higher total spins are responsible for the occurrence of negative conductances, we have studied the influence of spin relaxation with varying strength. Figure 2 shows specific numerical results

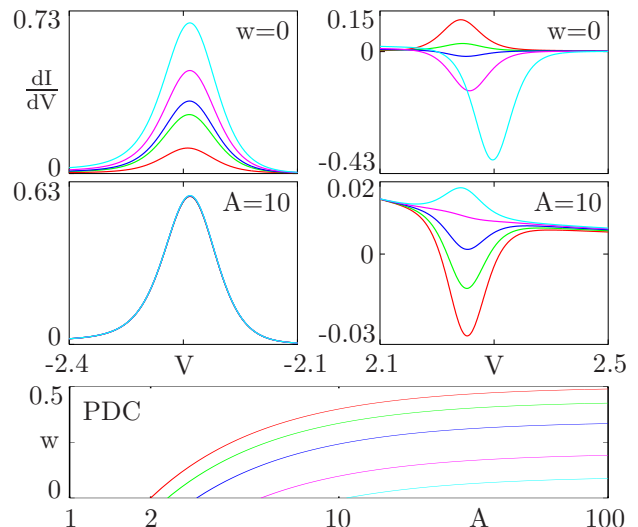


FIG. 2: Differential conductance (units  $e^2 \gamma_r / E_\sigma$ ) at positive voltages  $V$ , in units  $E_\sigma / e$  (right), near  $(100) \leftrightarrow (200)$ , and at  $-V$  (left), for  $g_\rho = 0.135$ ,  $g_\sigma = 1.25$  and  $g_0 = 0.9$ , at  $n_g$  in region I, with  $k_B T = 10^{-2} E_\sigma$ . Top panels:  $w = 0$ , with  $A = 1$  (red), 2 (green), 2.6 (blue), 5 (magenta) 50 (cyan). Middle:  $A = 10$  with  $w/\tilde{\gamma} = 0.3$  (red), 0.35 (green), 0.4 (blue), 0.45 (magenta), 0.5 (cyan). Bottom: phase diagram of the crossover between positive and negative conductance at  $T = 0$  for  $g_0 = 1$  (red), 0.9 (green), 0.8 (blue), 0.7 (magenta), 0.65 (cyan) for  $n_g$  in region I ( $w$  in units  $\tilde{\gamma} = \gamma_1(E_\sigma / \hbar \omega_c)^\alpha$ ).

for the differential conductance at positive and negative biases for  $n_g$  fixed in region I near the  $(100) \rightarrow (200)$  transition, when the asymmetry  $A$  (top panels) and the relaxation  $w$  (middle panels) are varied.

At  $w = 0$ , for small asymmetries, say  $A < 2$ , all peaks are positive. For larger asymmetries,  $A > 2$ , the peak corresponding to positive bias can become negative (top panels). At fixed asymmetry ( $A = 10$ , middle panels), by increasing the relaxation rate of the state  $(200)$  towards the intrinsic rate  $\tilde{\gamma} = \gamma_1(E_\sigma / \hbar \omega_c)^\alpha$ , the height of the negative conductance peak is reduced, while the corresponding positive conductance peak for  $V < 0$  is unchanged. When  $w \ll \tilde{\gamma}$ , the  $(200)$  state is stable and the negative conductance feature is strong. However, when  $w > \tilde{\gamma}/2$ , the  $(200)$  state becomes unstable in favor of  $(000)$  and the negative conductance vanishes since the ground state channels are re-opened.

For finite asymmetry,  $A > 1$ , and with spin relaxation,  $w > 0$ , one finds a finite critical value,  $A_c$ , for each negative conductance feature such that one gets  $G > 0$  for  $A < A_c$ . The critical trajectories  $w_c(A)$  for which the negative conductance peak disappears depends on the state with the highest spin  $s_{\text{max}} > 1$  involved in the transport, on the interaction strength in the leads, and on the relaxation. In the above example with  $s_{\text{max}} = 2$ ,  $w_c(A)$  is obtained by setting  $N = 0$  in Eq. (6) at the voltage corresponding to the position of the negative conductance peak and finite interaction in the leads. This phase tra-

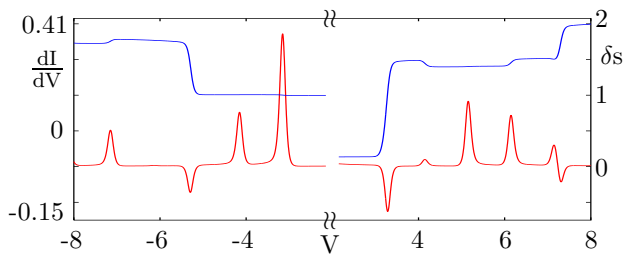


FIG. 3: Differential conductance (red curve, left scale, units  $e^2\gamma_r/E_\sigma$ ) and spin variance (blue curve, right scale) as a function of bias voltage  $V$  (unit  $E_\sigma/e$ ) for  $n_g$  in region I,  $A = 100$ ,  $w = 0$ ,  $k_B T = 2 \cdot 10^{-2} E_\sigma$ ,  $E_\rho = 25 E_\sigma$ ,  $\varepsilon_\sigma = 2.5 E_\sigma$ ,  $\varepsilon_\rho = 15 E_\sigma$ ,  $g_0 = 0.9$ .

jectory is shown in Fig. 2 (bottom) for different  $g_0$ . The negative conductance depends crucially on the interaction in the leads  $g_0$ . For decreasing  $g_0$  tunneling becomes less efficient, giving spin relaxation increased importance. However, *with interactions in the leads*, the negative conductance features, once they are stabilized, can even become enhanced as compared with their positive counterparts at negative voltages. Similar results are obtained for higher  $s_{\max}$ , but spin relaxation is then more efficient in preventing their formation,  $w_c(s_{\max} + 1) < w_c(s_{\max})$ .

Figure 3 shows the differential conductance and the spin fluctuations  $\delta s \equiv [\sum_{n,s} (s - \langle s \rangle)^2 P(n, s)]^{1/2}$  as a function of the bias for  $g_0 = 0.9$  with  $A = 100$ . The conductance shows positive and negative peaks for increasing bias (beyond the first two ground state peaks not shown here). One observes a step in the spin fluctuation near the negative conductance peaks. This is due to the participation of the higher-spin states in the transport. For example, the first negative peak at  $V = 2.3 E_\sigma/e$  in Fig. 3 contains mainly contributions from  $s = 2$ . Consequently, the spin variance jumps to a value dominated by  $P(n, s = 2)$ . This remains dominant even if new conductance channels enter (subsequent positive peaks). It changes only when the  $s = 4$  spin channel enters (second negative peak at about  $V = 7.3 E_\sigma/e$ ). Since we consider the transition  $n \leftrightarrow n + 1$  with  $n = \text{even}$ , we conclude that for positive voltage, *even* values of the spin dominate the spin dynamics. For negative voltages *odd* spins are dominant. Strong steps in  $\delta s$  are also found at the voltages of the positive conductance peaks with  $n_g$  in region III. This indicates that they are an intrinsic feature of the contribution to transport of the states with higher spins.

In conclusion, we have investigated the non-linear, sequential transport in a 1D non-Fermi liquid quantum dot embedded in a correlated electron system including spin. We have found that there are distinct negative differential conductances induced by spin-charge separation, if asymmetric tunnel barriers connect the quantum dot to the leads. We found that one can – *without applying a magnetic field* – stabilize states with higher total spins in certain regions of the parameter plane spanned by bias

and gate voltage if the asymmetry of the tunnel barriers exceeds a critical value depending on spin relaxation mechanisms competing with the non-Fermi liquid correlations. The participation in the transport of the states with higher total spins is indicated by the sensitivity to spin-flip relaxation and by strong changes in the spin fluctuations. The predicted phenomenon should occur in quasi-1D quantum dots containing even *many* electrons for spin states different from the ground state but *not* necessarily with maximum total spin. The physical origin of this new correlation-induced trapping phenomenon are the non-Fermi liquid properties of the system which lead to spin-charge separation and non-trivially enter the tunneling rates. The results in Fig. 2 show that the negative differential conductances are not restricted to very large asymmetry. Depending on the interaction parameters, they can occur also for moderate asymmetries of the order of 2 and even smaller. We expect that the above non-Fermi liquid phenomenon will be accessible using quasi-1D electron systems with moderately controllable tunnel contacts such as carbon nanotubes, and quasi-1D semiconductor quantum wires. For the latter, asymmetric barriers seem to us to be the genuine case.

Financial support of the EU via RTN FMRX-CT2000-00144 and the Italian MURST, PRIN02 is acknowledged.

- 
- [1] See, e.g. L.P. Kouwenhoven, *et al.*, in *Mesoscopic Electron Transport*, edited by L.L. Sohn, L.P. Kouwenhoven, and G. Schön (Kluwer, Dordrecht 1997).
  - [2] W. Liang, M. Bockrath, and H. Park, Phys. Rev. Lett. **88**, 126801 (2002).
  - [3] M. Buitelaar, *et al.*, Phys. Rev. Lett. **88**, 156801 (2002).
  - [4] D.H. Cobden, and J. Nygård, Phys. Rev. Lett. **89**, 046803 (2002).
  - [5] D. Weinmann, W. Häusler, and B. Kramer, Phys. Rev. Lett. **74**, 984 (1995).
  - [6] M. Ciorga, *et al.*, Phys. Rev. Lett. **88**, 256804 (2002).
  - [7] T. Fujisawa, *et al.*, Phys. Rev. Lett. **88**, 236802 (2002).
  - [8] O.M. Auslaender, *et al.*, Phys. Rev. Lett. **84**, 1764 (2000).
  - [9] A. Braggio, M. Sassetti, and B. Kramer, Phys. Rev. Lett. **87**, 146802 (2001); T. Kleimann, *et al.*, Phys. Rev. **B62**, 8144 (2000).
  - [10] O. M. Auslaender, *et al.*, Science **295**, 825 (2002).
  - [11] Y. Tserkovnyak, *et al.*, Phys. Rev. Lett. **89**, 136805 (2002); Phys. Rev. **B68**, 125312 (2003).
  - [12] Yu.V. Nazarov, and L.I. Glazman Phys. Rev. Lett. **91**, 126804 (2003).
  - [13] D.G. Polyakov, and I.V. Gornyi Phys. Rev. **B68**, 035421 (2003).
  - [14] J. Voit, Rep. Progr. Phys. **58**, 977 (1995).
  - [15] A. Furusaki, Phys. Rev. **B57**, 7141 (1998).
  - [16] J.U. Kim, I.V. Krive, and J.M. Kinaret, Phys. Rev. Lett. **90**, 176401 (2003).
  - [17] A. V. Khaetskii and Yu.V. Nazarov, Phys. Rev. **B64**, 125316 (2001).